Dominance of many-body effects over one-electron mechanism for band structure doping dependence in $Nd_{2-x}Ce_xCuO_4$: LDA+GTB approach

M M Korshunov[1,2], V A Gavrichkov[1], S G Ovchinnikov[1], I A Nekrasov[3], E E Kokorina[3], Z V Pchelkina[4]

[1] L.V. Kirensky Institute of Physics, Siberian Branch of Russian Academy of Sciences, 660036 Krasnoyarsk, Russia

[2] Max-Planck-Institut für Physik komplexer Systeme, D-01187 Dresden, Germany

[3] Institute of Electrophysics, Russian Academy of Sciences-Ural Division, 620016 Yekaterinburg, Amundsena 106, Russia

[4] Institute of Metal Physics, Russian Academy of Sciences-Ural Division, 620041 Yekaterinburg, GSP-170, Russia

E-mail: `maxim@mpipks-dresden.mpg.de`

Abstract. In the present work we report band structure calculation of high temperature superconductor $Nd_{2-x}Ce_xCuO_4$ in the regime of strong electronic correlations within LDA+GTB method, which combines local density approximation (LDA) and generalized tight-binding method (GTB). Two mechanisms of band structure doping dependence were taken into account: one-electron and many-body ones. We have shown that in the antiferromagnetic and a strongly correlated paramagnetic phases of the underdoped cuprates the main contribution to the doping evolution of the band structure is provided by the many-body mechanism.

PACS numbers: 71.27.+a, 74.25.Jb, 71.18.+y

Submitted to: *J. Phys.: Condens. Matter*

1. Introduction

It is well known that hole doping of $La_{2-x}Sr_xCuO_4$ and electron doping of $Nd_{2-x}Ce_xCuO_4$ shifts them into superconducting state. With the increase of doping concentration x the band structure undergoes dramatic changes from antiferromagnetic (AFM) dielectric type to a normal paramagnetic metal. It is well established that strong electronic correlations play one of the main roles in the forming of electronic structure of High-T_c cuprates. They are important especially for small x values and should be taken into account in the calculations explicitly.

In the present paper to study $Nd_{2-x}Ce_xCuO_4$ band structure we apply the LDA+GTB hybrid computational scheme [1], which combines the many-body generalized tight-binding approach [2] and *ab-initio* LDA calculations. Earlier within GTB method the specific many-body mechanism of band structure evolution for doped Mott-Hubbard insulators was revealed. This mechanism is caused by changes of occupation factors of many-body electronic terms by quasiparticle excitations [2]. For $Nd_{2-x}Ce_xCuO_4$ such terms are $d^{10}p^6$ (zero holes per cell) and hybridized term $d^9p^6+d^{10}p^5$ (one hole per cell). In this paper we highlight also the so called "one-electron" mechanism of band structure doping dependence. It appears from the changes of crystal structure (lattice parameters, atomic positions) upon doping. As a result matrix elements of $d-d$, $p-d$ and $p-p$ hybridization (hopping) and all the rest which depend on interatomic distance vary with doping. In case of absence of a strong electronic correlations this mechanism will be responsible for evolution of band structure with doping in the framework of standard band theory. That is why we call it one-electron mechanism.

To our knowledge there is no calculation of band structure of High-T_c cuprates allows for both mechanisms. In this paper we report the results of such calculations for $Nd_{2-x}Ce_xCuO_4$ and compare them with the simplified calculation without consideration of one-electron mechanism. It was found that in the antiferromagnetic region for small doping $x \leq 0.1$ one-electron mechanism results in a slight shift of the bottom of conduction band and, simultaneously, in a slight shift of the top of a valence band, thus retaining the value of the charge-transfer gap. For higher doping concentration the paramagnetic spin-liquid phase was considered in an approximation taking the static spin-spin correlation functions into account. In this phase one-electron mechanism provided small changes in the bandwidth, but the Fermi surface and concentrations of its topology changes remain the same as in the case of no-presence of the one-electron mechanism.

2. Brief description of a hybrid LDA+GTB computational scheme

Ab-initio electronic structure calculations within the density functional theory have their development in the LDA approximation. This approximation does not take into account strong electronic correlations properly, that is why true band structure of Mott insulators

can not be described within LDA. We employ LDA to calculate the non-interacting part of the multi-band $p-d$ model Hamiltonian, where strong electronic correlations enters in the framework of the GTB approach [1].

LDA+GTB method consists of following steps:

(i) *Ab-initio* LDA band structure calculation, finding of Bloch functions;

(ii) Construction of the Wannier functions for physically relevant states;

(iii) Construction of the multi-band $p-d$ model Hamiltonian with parameters obtained from the previous two steps;

(iv) Splitting of the multi-band $p-d$ model Hamiltonian into a sum of inter- and intra-cell components and exact diagonalization of intra-cell part in order to construct the many-body molecular orbitals of the cell;

(v) Construction of intra-cell Hubbard X-operators on the basis of these orbitals and rewriting the full Hamiltonian for the crystal in the X-representation;

(vi) Calculation of a quasiparticle band structure for Hubbard fermions in the framework of the perturbation theory with small inter-cell hopping and interactions.

Note, the first version of the GTB method [2, 3] contained large number of unknown model parameters, which were extracted from the comparison of different calculations with experimental data. In the generalized LDA+GTB method all parameters of the theory are calculated explicitly. For a given doping concentration x we calculate *ab-initio* band structure. One-electron mechanism of band structure doping dependence is determined by the dependence of matrix elements of the inter-atomic hopping and one-electron energies on doping, which is due to the difference of the lattice parameters for different x. Many-body mechanism arises from the doping dependence of the occupation factors. Thus, one-electron mechanism takes place for the ordinary tight-binding method, while the many-body mechanism appears within the GTB method as the effect of strong electronic correlations.

3. Electronic structure and model parameters of $Nd_{2-x}Ce_xCuO_4$: LDA results

Nd_2CuO_4 crystallizes in tetragonal structure with symmetry space group I4/mmm [4], also called T'-structure. Lattice parameters are $a = b = 3.94362$Å, $c = 12.1584$ Å[4]. Cu ions in positions $2a$ $(0, 0, 0)$ are surrounded by four ions of oxygen O1, which occupy positions $4c$ $(0, 0.5, 0)$. Ions of Nd in positions $4e$ $(0, 0, 0.35112)$ have eight nearest neighbors of oxygen O2 in positions $4d$ $(0, 0.5, 0.25)$. In comparison with high-temperature tetragonal structure of La_2CuO_4, in T'-structure of Nd_2CuO_4 the apical oxygen ions around Cu ions are absent. With cerium doping the symmetry group of $Nd_{2-x}Ce_xCuO_4$ remains the same whereas the lattice parameters and z coordinate of neodymium positions are changing (see Table 1) [4, 5].

Electronic structure of $Nd_{2-x}Ce_xCuO_4$ at $0 \leq x \leq 0.3$ was calculated using the local density approximation (LDA). To this end the linearized muffin-tin orbitals (LMTO)

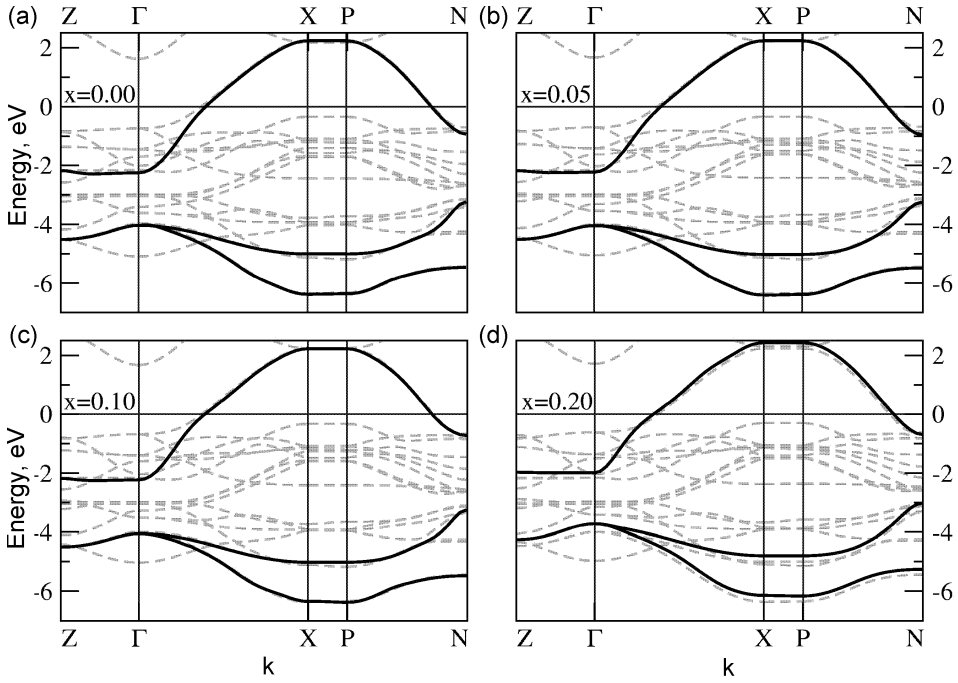

Figure 1. The comparison of electronic dispersions obtained within LDA calculations (gray dashed lines) and the one of effective non-interacting 3-band Hamiltonian constructed in the NMTO orbitals basis set (black solid lines) for different Ce concentrations.

Table 1. Crystal structure parameters (Å) for $Nd_{2-x}Ce_xCuO_4$ for different Ce concentrations (see Refs. [4, 5]).

Lattice constant	$x = 0.00$	0.05	0.10	0.15	0.20	0.30
a	3.94362	3.94056	3.94071	3.94224	3.94295	3.94288
c	12.1584	12.1130	12.0945	12.0603	12.030	12.0288
z(Nd)	0.35112	0.3519	0.3523	0.3527	0.3531	0.3531

method in the tight-binding approach within atomic spheres approximation (TB-LMTO-ASA) was applied [6, 7]. In the calculations the $4f$ states of Nd were considered as semi-core states, because they are well localized and situated far below the d states [8]. The LDA band structure of $Nd_{2-x}Ce_xCuO_4$ along the high symmetry directions of the Brillouin zone is shown on Fig. 1 with gray dashed lines. Bands formed by the hybridized $3d$ copper and $2p$ oxygen states has a width of approximately 9 eV. As a result of hybridization between $d_{x^2-y^2}$ copper orbital and appropriate $p_{x,y}$ orbitals of plain oxygen (O1) the bonding bands are located at energies $-5...-6$ eV and antibonding band crosses the Fermi level. The hybrid orbitals mentioned above determine the non-interacting Hamiltonian of the so-called 3-band $p-d$ model [9, 10].

To calculate hopping integrals for the 3-band $p-d$ model the NMTO (muffin-tin orbitals of N-th order) [11] method was used. For these three physically relevant hybrid bands the NMTO orbitals were constructed. Corresponding band dispersions

Table 2. Values of hopping integrals and one-electron energies (eV) as a function of Ce concentration for $Nd_{2-x}Ce_xCuO_4$ obtained by the NMTO method. Here x^2, p_x, p_y denote the Cu-$d_{x^2-y^2}$ and O1-$p_{x,y}$ orbitals respectively.

		$x = 0.00$	0.05	0.10	0.15	0.20	0.30
Energy							
$E(x^2)$		-2.2855	-2.2847	-2.1760	-2.4215	-2.3507	-2.3234
$E(p_x)$		-3.2935	-3.3064	-3.2829	-3.2607	-3.2800	-3.2957
Hopping	Direction						
$t(x^2, p_x)$	(0.5, 0)	1.1216	1.1454	1.1665	1.1614	1.1726	1.1719
$t'(x^2, p_x)$	(0.5, 1)	-0.0504	-0.0359	-0.0211	-0.0202	-0.0166	-0.0201
$t''(x^2, p_x)$	(1.5, 0)	0.0834	0.0921	0.1173	0.1130	0.1203	0.1126
$t'''(x^2, p_x)$	(1.5, 1)	-0.0149	-0.0083	0.0015	0.0090	0.0153	0.0099
$t(p_x, p_y)$	(0.5, 0.5)	0.8320	0.8389	0.8381	0.8365	0.8386	0.8304
$t'(p_x, p_y)$	(1.5, 0.5)	0.0266	0.0331	0.0452	0.0450	0.0469	0.0388

are shown in Fig. 1 by solid black lines. It is seen that NMTO orbitals are almost perfectly reproduce the LDA calculated bonding and antibonding bands formed by a hybrid $d_{x^2-y^2}$ copper and $p_{x,y}$ oxygen orbitals. Thus, within this NMTO basis we have obtained an effective few-orbital Hamiltonian, the 3-band $p-d$ model, which we were looking for.

Having applied the Fourier transform to this effective Hamiltonian in momentum space we obtain real space hopping integrals depending on distances between atoms (see Table 2). From Fig. 1 and Table 2 one can conclude that hopping integrals change slightly with doping. It allows us to assume that the one-electron contribution to the evolution of $Nd_{2-x}Ce_xCuO_4$ electronic structure with increase of cerium concentration is not substantial.

For the 3-band $p-d$ model we also need the values of Coulomb repulsion U and Hund's exchange parameter J_H for Cu ions. In the paper [12] they were calculated for copper in the La_2CuO_4 compound by a super-cell method [13] and equal to: $U = 10$ eV, $J_H = 1$ eV. We presume these values to be doping independent and use them in the present paper for the $Nd_{2-x}Ce_xCuO_4$ compound.

4. LDA+GTB results in AFM phase

In the wide range of doping concentrations $Nd_{2-x}Ce_xCuO_4$ remains in AFM phase. Therefore we will consider the evolution of band structure with doping in the AFM phase first. Within the GTB method for this phase we use the Hubbard-I approximation [14], though the diagram technique for the X-operators [15, 16, 17] allows one to go beyond this approximation.

To write down the model Hamiltonian we use the Hubbard X-operators [18]: $X_f^{\alpha} \leftrightarrow X_f^{n,n'} \equiv |n\rangle\langle n'|$. Here index $\alpha \leftrightarrow (n, n')$ enumerates quasiparticle with

energy $\omega_\alpha = \varepsilon_n(N+1) - \varepsilon_{n'}(N)$, where ε_n is the n-th energy level of the N-electron system. The commutation relations between X-operators are quite complicated, i.e. two operators commute on another operator, not a c-number. Nevertheless, depending on the difference of the number of fermions in states n and n' it is possible to define quasi-Fermi and quasi-Bose type operators in terms of obeyed statistics. There is a simple correspondence between X-operators and single-electron annihilation operators: $a_{f\lambda\sigma} = \sum\limits_{\alpha} \gamma_{\lambda\sigma}(\alpha) X_f^{\alpha}$, where the coefficients $\gamma_{\lambda\sigma}(\alpha)$ determines the partial weight of the quasiparticle α with spin σ and orbital index λ. These coefficients are calculated straightforwardly within the GTB scheme.

In the Hubbard-I approximation dispersion equation for the band structure of Hubbard fermions in the AFM phase with sublattices A and B, which corresponds to the ground state of underdoped La_2CuO_4 and Nd_2CuO_4, is the following [3]:

$$\left\| \left(E - \Omega_\alpha^B\right) \delta_{\alpha\beta}/F_\alpha^B - 2\sum_{\lambda\lambda'} \gamma_{\lambda\sigma}^*(\alpha) T_{\lambda\lambda'}^{AB}(\vec{k}) \gamma_{\lambda'\sigma}(\beta) \right\| = 0, \qquad (1)$$

where Ω_α^B is the intra-cell local energy of the Hubbard's fermion, $T_{\lambda\lambda'}^{AB}(\vec{k})$ is the Fourier transform of the matrix element of intra-cell hopping between one-electron orbitals λ and λ'. The occupation factor F_α^B is equal to the sum of the occupancies of initial and final many-body states, the transition between which is described by the operator X_f^α.

Since the structure of dispersion equation (1) is similar to the equation in the one-electron tight-binding approach our method was called Generalized Tight-Binding (GTB) method. At the same time there are important distinctions of equation (1) from its one-electron analogue. Namely, the local energies Ω_α^B are calculated with explicit consideration of strong electronic correlations inside the cell. Thus, corresponding occupation factor can have non-integer values and depend on temperature and doping concentration. As a result, the doping dependence of the electronic structure is not described by the rigid band model, so the effect of doping is not only due to the shift of a chemical potential for a given band structure. On the contrary, the band structure is unique for each doping concentration x, and with doping the new bands appear. Their spectral weight at small doping is proportional to x. Such bands appear, for example, inside the dielectric gap near of the bottom of the conduction band for n-type cuprates and near of the top of the valence band in hole-doped cuprates. These states are called "in-gap states" [2, 3, 19]. Note, these states are not an impurity states of a doped semiconductor formed in the presence of a defect since no defects are present in our model. An example of the in-gap states near of the bottom of conduction band in $Nd_{2-x}Ce_xCuO_4$ will be discussed later in this section.

The results of the LDA+GTB calculations of dispersion dependences given by the equation (1) in the Neel state of a doped compound are shown in Fig. 2. In each figure the results for a given doping concentration of two calculations are shown: (i) with parameters calculated for $x = 0$ (i.e. in absence of one-electron mechanism but taking into account many-body mechanism), and (ii) for the model parameters depending on the concentration (see Table 2), also taking into account the many-body mechanism.

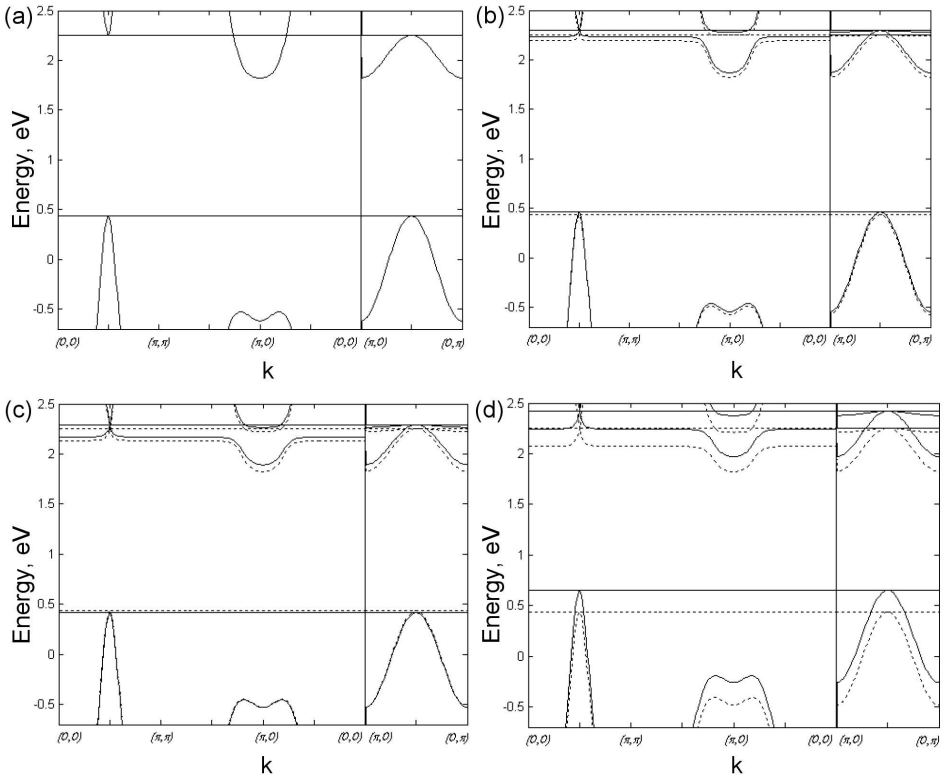

Figure 2. Quasiparticle's energy momentum dependences calculated within LDA+GTB method for the following concentrations: (a) $x = 0$, (b) 0.05, (c) 0.1, (d) 0.15. The dotted line corresponds to the calculations without taking into account one-electron mechanism of concentration dependence. The solid line represents results of calculations in which both many-body and one-electron mechanisms were considered.

In the former case doping dependence was determined only by the doping-dependent occupation factors F_α^B, while in the latter case the dependence of matrix elements $T_{\lambda\lambda'}^{AB}(\vec{k})$ on doping was taken into account.

The results of electronic structure calculations for an undoped compound (Fig. 2(a)) reproduce the main effects of strong electronic correlations in that material. On the bottom of conduction band and on the top of valence band there are in-gap states with the spectral weight proportional to the doping level [2, 3, 19]. Upon increase of doping concentration the in-gap states at the bottom of conduction band become dispersive with non-zero spectral weight (see Fig. 2(b-d)).

For each concentration one can notice that "switching-off" of the one-electron mechanism leads to a shift of the top of valence band and the bottom of conduction band. This shift is almost uniform and its value is very small. Also, they do not prevent appearance of the in-gap states. Thus, one can conclude that such fine tuning of Hamiltonian parameters taking into account their doping dependence gives just a shift of electronic structure as a whole in the vicinity of the dielectric gap. This is most probably not important for the physics of High-T_c materials.

5. Paramagnetic phase

To treat spin-liquid phase the multiband $p-d$ model Hamiltonian was mapped onto an effective low-energy model [1]. Parameters of this effective model are obtained directly from the *ab-initio* parameters of the multiband model. The low-energy model for n-type cuprates is the $t-t'-t''-J^*$ model ($t-t'-t''-J$ model with the three-site correlated hoppings) with the following Hamiltonian in the hole representation:

$$H = \sum_{f,\sigma} (\varepsilon_0 - \mu) X_f^{\sigma,\sigma} + \sum_{f\neq g,\sigma} t_{fg} X_f^{\sigma,0} X_g^{0,\sigma} + \sum_{f\neq g} J_{fg} \left(\vec{S}_f \vec{S}_g - \frac{1}{4} n_f n_g \right) + H_3. \quad (2)$$

Here μ is the chemical potential, $\vec{S}_f$ is the spin operator, $S_f^+ = X_f^{\sigma,\bar{\sigma}}$, $S_f^- = X_f^{\bar{\sigma},\sigma}$, $S_f^z = \frac{1}{2}\left(X_f^{\sigma,\sigma} - X_f^{\bar{\sigma},\bar{\sigma}}\right)$, $n_f = \sum\limits_{\sigma} X_f^{\sigma,\sigma}$ is the number of particles operator, $J_{fg} = 2\tilde{t}_{fg}^2/E_{ct}$ is the exchange parameter, E_{ct} is the charge-transfer gap. In the notations of Ref. [1] the hopping matrix elements t_{fg} corresponds to $-t_{fg}^{00}$, and $\tilde{t}_{fg} = t_{fg}^{0S}$. Hamiltonian H_3 contains the three-site interaction terms:

$$H_3 = \sum_{f\neq g\neq m,\sigma} \frac{\tilde{t}_{fm}\tilde{t}_{mg}}{E_{ct}} \left(X_f^{\sigma 0} X_m^{\bar{\sigma}\sigma} X_g^{0\bar{\sigma}} - X_f^{\sigma 0} X_m^{\bar{\sigma}\bar{\sigma}} X_g^{0\sigma} \right). \quad (3)$$

In the considered case there is only one quasi-Fermi-type quasiparticle, $\alpha = (0,\sigma)$, with $\gamma_{\lambda\sigma}(\alpha) = 1$, and the Hamiltonian in the generalized form in momentum representation is given by:

$$H = \sum_{\vec{k},\sigma} (\varepsilon_0 - \mu) X_{\vec{k}}^{\sigma,\sigma} + \sum_{\vec{k}} \sum_{\alpha,\beta} t_{\vec{k}}^{\alpha\beta} X_{\vec{k}}^{\alpha\dagger} X_{\vec{k}}^{\beta} + \sum_{\vec{p},\vec{q}} \sum_{\alpha,\beta,\sigma,\sigma'} V_{\vec{p}\vec{q}}^{\alpha\beta,\sigma\sigma'} X_{\vec{p}}^{\alpha\dagger} X_{\vec{p}-\vec{q}}^{\sigma,\sigma'} X_{\vec{q}}^{\beta}. \quad (4)$$

The Fourier transform of the two-time retarded Green function in the energy representation, $G_\lambda(\vec{k},E) = \left\langle\left\langle a_{\vec{k}\lambda\sigma} \middle| a_{\vec{k}\lambda\sigma}^\dagger \right\rangle\right\rangle_E$, can be rewritten in terms of the matrix Green function $\left[\hat{D}(\vec{k},E)\right]_{\alpha\beta} = \left\langle\left\langle X_{\vec{k}}^{\alpha} \middle| X_{\vec{k}}^{\beta\dagger} \right\rangle\right\rangle_E$:

$$G_\lambda(\vec{k},E) = \sum_{\alpha,\beta} \gamma_{\lambda\sigma}(\alpha)\gamma_{\lambda\sigma}^*(\beta) D^{\alpha\beta}(\vec{k},E). \quad (5)$$

The generalized Dyson equation for the Hubbard X-operators [17] in the paramagnetic phase ($\langle X_0^{\sigma,\sigma}\rangle = \left\langle X_0^{\bar{\sigma},\bar{\sigma}}\right\rangle$) reads:

$$\hat{D}(\vec{k},E) = \left[\hat{G}_0^{-1}(E) - \hat{P}(\vec{k},E)\hat{t}_{\vec{k}} - \hat{P}(\vec{k},E)\hat{V}_{\vec{k}\vec{k}}^{\sigma,\sigma} \langle X_0^{\sigma,\sigma}\rangle + \hat{\Sigma}(\vec{k},E)\right]^{-1} \hat{P}(\vec{k},E). \quad (6)$$

Here, $\hat{G}_0^{-1}(E)$ is the exact local Green function, $G_0^{\alpha\beta}(E) = \delta_{\alpha\beta}/\left[E - (\varepsilon_n - \varepsilon_{n'})\right]$, $\hat{\Sigma}(\vec{k},E)$ and $\hat{P}(\vec{k},E)$ are the self-energy and the strength operators, respectively. The presence of the strength operator is due to the redistribution of the spectral weight between the Hubbard subbands, that is an intrinsic feature of the strongly correlated electron systems. It also should be stressed that $\hat{\Sigma}(\vec{k},E)$ in Eq. (6) is the self-energy in X-operators representation and therefore it differs from the self-energy entering Dyson equation for the weak coupling perturbation theory for $G_\lambda(\vec{k},E)$.

To calculate strength operator $\hat{P}(\vec{k},E)$ we use zero-loop approximation given by the replacement $P^{\alpha\beta}(\vec{k},E) \to P^{\alpha\beta} = \delta_{\alpha\beta}F_\alpha$, where $F_{\alpha(n,n')} = \left\langle X_f^{n,n}\right\rangle + \left\langle X_f^{n',n'}\right\rangle$ is the

occupation factor. Taking into account that in the considered paramagnetic phase $\left\langle X_f^{\sigma,\sigma}\right\rangle = \frac{1-x}{2}$, $\left\langle X_f^{0,0}\right\rangle = x$, after all substitutions and treating all $\vec{k}$-independent terms as the chemical potential renormalization, the generalized Dyson equation for the Hamiltonian (2) becomes:

$$D(\vec{k},E) = \frac{(1+x)/2}{E-(\varepsilon_0-\mu)-\frac{1+x}{2}t_{\vec{k}}-\frac{1+x}{2}\frac{\tilde{t}^2_{\vec{k}}}{E_{ct}}\frac{1-x}{2}+\Sigma(\vec{k},E)}. \tag{7}$$

To go beyond the Hubbard-I approximation we have to calculate $\Sigma(\vec{k},E)$. This was done in Ref. [20] using an equations of motion method for the X-operators [21] and resulted in the following expression:

$$\Sigma(\vec{k}) = \frac{2}{1+x}\frac{1}{N}\sum_{\vec{q}}\left\{\left[t_{\vec{q}}-\frac{1-x}{2}J_{\vec{k}-\vec{q}}-x\frac{\tilde{t}^2_{\vec{q}}}{E_{ct}}-\frac{1+x}{2}\frac{2\tilde{t}_{\vec{k}}\tilde{t}_{\vec{q}}}{E_{ct}}\right]K_{\vec{q}}\right.$$
$$\left.-\left[t_{\vec{k}-\vec{q}}-\frac{1-x}{2}\left(J_{\vec{q}}-\frac{\tilde{t}^2_{\vec{k}-\vec{q}}}{E_{ct}}\right)-\frac{1+x}{2}\frac{2\tilde{t}_k\tilde{t}_{\vec{k}-\vec{q}}}{E_{ct}}\right]\frac{3}{2}C_{\vec{q}}\right\}. \tag{8}$$

Here N is the number of vectors in momentum space, and also static spin-spin correlation functions

$$C_{\vec{q}} = \sum_{f,g} e^{-i(f-g)\vec{q}}\left\langle X_f^{\sigma\bar{\sigma}}X_g^{\bar{\sigma}\sigma}\right\rangle = 2\sum_{\vec{r}} e^{-i\vec{r}\vec{q}}\left\langle S^z_{\vec{r}}S^z_0\right\rangle, \tag{9}$$

and kinematic correlation functions

$$K_{\vec{q}} = \sum_{f,g} e^{-i(f-g)\vec{q}}\left\langle X_f^{\sigma 0}X_g^{0\sigma}\right\rangle, \tag{10}$$

were introduced.

Kinematic correlation functions (10) are calculated straightforwardly with the help of Green function (7). The spin-spin correlation functions for the $t-J$ model with three-site correlated hoppings H_3 were calculated in Ref. [22] and the following expression for the Fourier transform of the spin-spin Green function was derived:

$$\left\langle\left\langle X^{\sigma\bar{\sigma}}_{\vec{q}} \mid X^{\bar{\sigma}\sigma}_{\vec{q}}\right\rangle\right\rangle_\omega = \frac{A_{\vec{q}}(\omega)}{\omega^2-\omega^2_{\vec{q}}}, \tag{11}$$

where $A_{\vec{q}}(\omega)$ and magnetic excitations spectrum $\omega_{\vec{q}}$ are given in Ref. [22] by the Eqs. (25) and (26), respectively.

The following results were obtained by self-consistent calculation of the chemical potential μ, the spin-spin correlation functions (9) using Green function (11), and the kinematic correlation functions (10) using Green function (7) with the self-energy (8).

Our results for the doping dependence of the kinematic and spin-spin correlation functions are shown in Fig. 3. Note, the behavior of all correlation functions is almost identical in the cases of presence and absence of one-electron mechanism of doping dependence. Also note, the kinematic correlation functions K_n possess a very nontrivial doping dependence. For low concentrations, $x < 0.2$, due to the strong magnetic correlations the hoppings to the nearest neighbors are suppressed leading to the small value of K_1, while K_2 and K_3 are not suppressed. Upon increase of the doping

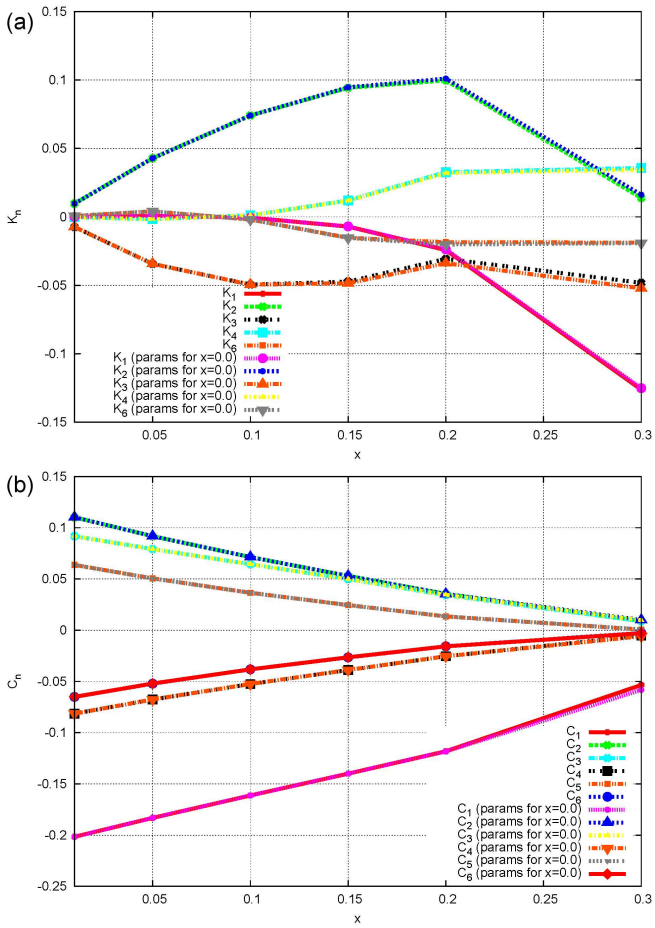

Figure 3. (color online) Doping dependent evolution of the kinematic (a) and spin-spin (b) correlation functions within the $t - t' - t'' - J^*$ model. Index n enumerates real space vectors connecting neighboring sites: $n = 1$ for nearest-neighbors, $n = 2$ for the next nearest neighbors, and so on.

concentration above $x \approx 0.2$, magnetic correlations decrease considerably and nearest-neighbor kinematic correlation function K_1 increase, reviving the almost Fermi liquid behavior: K_1 becomes largest of all K_n's, while the magnetic correlation functions C_n are strongly suppressed.

So, we can clearly define one point of the crossover, namely $x_m \approx 0.2$. The system behavior is quite different on the different sides of these points, although there is no phase transition with symmetry breaking occurs. Apparently, this crossover is closely connected to the changes in the Fermi surface topology with doping. This evolution together with the quasiparticle dispersion is shown in Fig. 4. For small x the electron pockets around $(\pm\pi, 0)$ and $(0, \pm\pi)$ points are present at the Fermi surface. Upon increase of the doping concentration these pockets become larger and merge together at $x = 0.2$. For higher concentrations the FS appear to be a large hole-like one, shrinking toward (π, π) point. Thus, the topology of the Fermi surface changes at the same doping as the point of crossover x_m takes place. For the first time the "electronic

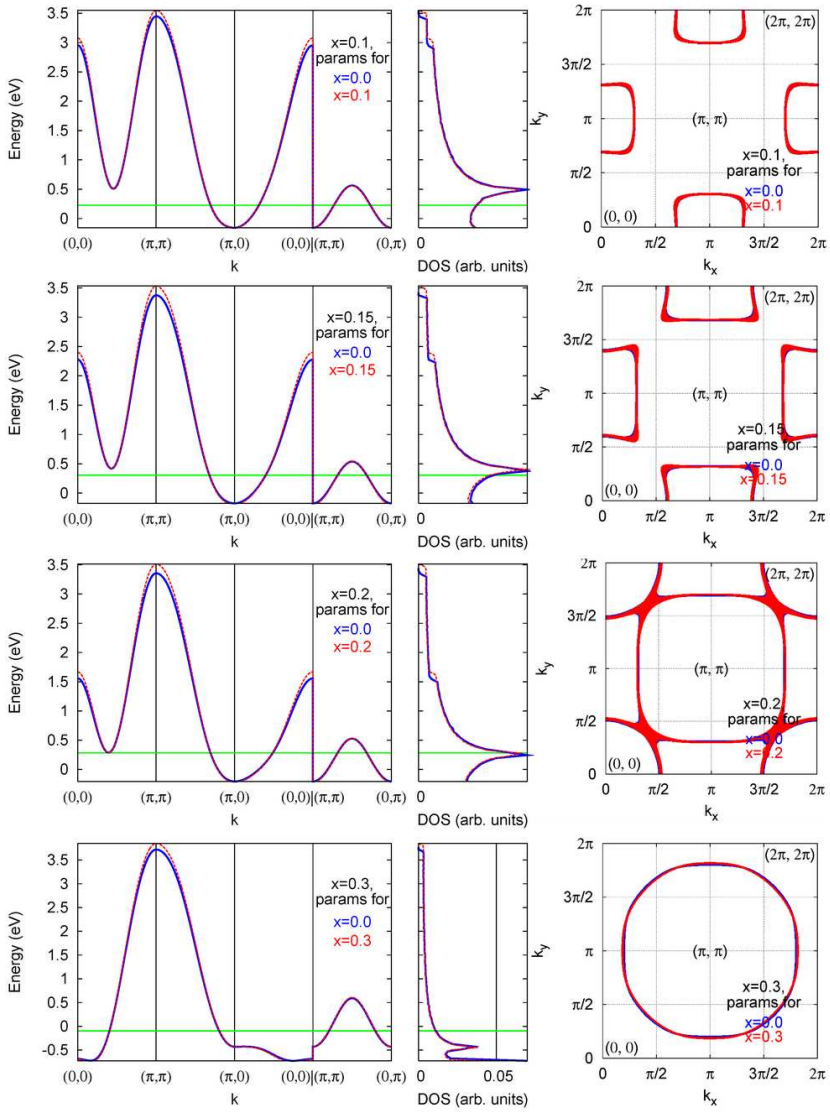

Figure 4. Doping-dependent quasiparticle dispersion (on the left) and Fermi surface (on the right) in the spin-liquid phase of n-type cuprate are presented. The position of the chemical potential is denoted by the horizontal (green) line. The solid blue lines corresponds to the calculations without taking into account one-electron mechanism of concentration dependence. The dashed red lines represents results of calculations in which both many-body and one-electron mechanisms were considered.

transition" accompanying the change in the Fermi surface topology, or the so-called Lifshitz transition, was described in Ref. [23]. Now such transitions referred as a quantum phase transitions with a co-dimension= 1 (see e.g. paper [24]).

Note, when the Fermi surface topology changes at a quantum critical concentration $x_m = 0.2$ the density of states at the Fermi level also exhibit significant transformations. This results in the different behavior of the kinematic and magnetic correlation functions on the different sides of this crossover point. And, of course the changes in the density of states at the Fermi level will also result in the significant changes of such observable

physical quantities as the resistivity and the specific heat.

Concerning the role of the short range magnetic order and three-site hopping terms in n-type cuprates we would like to stress that due to the scattering on the magnetic excitations with AFM wave vector $\vec{Q} = (\pi, \pi)$ the states near the (π, π) point pushed above the Fermi level, and the local symmetry around the $(\pi/2, \pi/2)$ points is restored for low doping concentrations (see Fig. 4). In other words, the short range magnetic order "tries" to restore the AFM symmetry around $(\pi/2, \pi/2)$ point. In our calculations the short range magnetic fluctuations are taken into account via the spin-spin correlation functions (9).

Now we proceed to the comparison of the one-electron and many-body mechanisms of doping dependence. In Fig. 4 the quasiparticle dispersion without one-electron mechanism is shown by solid blue lines. Apparently, its difference from the case when both one-electron and many-body mechanisms are present is negligibly small. In the latter case the bandwidth is slightly renormalized while band dispersion retains the same character. Moreover, the Fermi surfaces for both cases are very similar. Thus, the quantum phase transition will be at the same concentration $x_m = 0.2$.

6. Conclusion

In present work we report the combined investigation of the one-electron and many-body mechanisms of electronic structure doping dependence for the High-T_c compound $Nd_{2-x}Ce_xCuO_4$. The electronic structure calculations were performed within the hybrid LDA+GTB scheme. In both antiferromagnetic and paramagnetic spin-liquid phases we demonstrate that the main effect to the electronic structure is provided by the many-body mechanism, whereas the one-electron contribution leads to rather small quantitative modifications which do not change the picture qualitatively. The role of many-body mechanism is very important because of the strong electronic correlations present in the underdoped cuprates.

Acknowledgments

This work was supported in part by RFBR Grants 06-02-16100 (M.M.K., V.A.G., S.G.O.), 06-02-90537-BNTS (M.M.K., V.A.G., S.G.O., I.A.N., Z.V.P.), 05-02-16301 (I.N.), 05-02-17244 (I.N.), by the joint UrO-SO project 74, and programs of the Presidium of the Russian Academy of Sciences (RAS) "Quantum macrophysics" and of the Division of Physical Sciences of RAS "Strongly correlated electrons in semiconductors, metals, superconductors and magnetic materials". M.M.K. acknowledge support form INTAS (YS Grant 05-109-4891). I.N. and Z.P. acknowledge support from the Dynasty Foundation and International Center for Fundamental Physics in Moscow program for young scientists. I.N. appreciate the support from the grant of President of Russian Federation for young PhD MK-2242.2007.02. Z.V. is supported by UrO grant for young scientists.

References

[1] Korshunov M M, Gavrichkov V A, Ovchinnikov S G, Nekrasov I A, Pchelkina Z V, Anisimov V I 2005 *Phys. Rev.* B **72** 165104

[2] Gavrichkov V A, Ovchinnikov S G, Borisov A A, Goryachev E G 2000 *Zh. Eksp. Teor. Fiz.* **118** 422 [*JETP* **91** 369]

[3] Gavrichkov V A, Ovchinnikov S G 2004 *Zh. Eksp. Teor. Fiz.* **125** 630 [*JETP* **98** 556]

[4] Kamiyama T, Izumi F, Takahashi H, Jorgensen J D, Dabrowski B, Hitterman R L, Hinks D G, Shaked H, Mason T O, Seabaugh M 1994 *Physica* C **229** 377

[5] Paulus E F, Yehia I, Fuess H, Rodriguez J, Vogt T, Ströbel J, Klauda M, Saemann-Ischenko G 1990 *Solid State Commun.* **73** 791

[6] Andersen O K, Jepsen O 1984 *Phys. Rev. Lett.* **53** 2571

[7] Andersen O K, Pawlowska Z, Jepsen O 1986 *Phys. Rev.* B **34** 5253

[8] Singh D J 1991 *Phys. Rev.* B **44** 7451

[9] Emery V J 1987 *Phys. Rev. Lett.* **58** 2794

[10] Varma C M, Smitt-Rink D, Abrahams E 1987 *Solid State Commun.* **62** 681

[11] Andersen O K, Saha-Dasgupta T 2000 *Phys. Rev.* B **62** 16219(R)

[12] Anisimov V I, Korotin M A, Nekrasov I A, Pchelkina Z V, Sorella S 2002 *Phys. Rev.* B **66** 100502

[13] Gunnarsson O, Andersen O K, Jepsen O, Zaanen J 1989 *Phys. Rev.* B **39** 1708

[14] Hubbard J C 1963 *Proc. R. Soc.* A **276** 238

[15] Zaitsev R O 1975 *Sov. Phys. JETP* **41** 100

[16] Izumov Yu, Letfullov B M 1991 *J. Phys.: Condens. Matter* **3** 5373

[17] Ovchinnikov S G, Val'kov V V 2004 *Hubbard Operators in the Theory of Strongly Correlated Electrons* (Imperial College Press, London-Singapore)

[18] Hubbard J C 1964 *Proc. R. Soc.* A **277** 237

[19] Ovchinnikov S G, Borisov A A, Gavrichkov V A, Korshunov M M 2004 *J. Phys.: Condens. Matter* **16** L93

[20] Korshunov M M, Ovchinnikov S G 2006 *cond-mat*/0610580

[21] Plakida N M, Yushankhai V Yu, Stasyuk I V 1989 *Physica* C **162-164** 787

[22] Val'kov V V, Dzebisashvili D M 2005 *Zh. Eksp. Teor. Fiz.* **127** 686 [*JETP* **100** 608]

[23] Lifshitz I M 1960 *Sov. Phys. JETP* **11** 1130

[24] Volovik G E 2006 *Acta Phys. Slov.* **56** 49; *cond-mat*/0601372

[25] Plakida N M, Oudovenko V S 2006 *cond-mat*/0606557 (to appear in Physica C)

[26] Plakida N M, Oudovenko V S 2007 *Zh. Eksp. Teor. Fiz.* **131** 259 [*JETP* **104** 230]